Overpotential-Based Battery End-of-Life Indication in WSN Nodes

Thomas Menzel and Adam Wolisz

Telecommunication Networks Group, TU Berlin, Einsteinufer 25, 10587 Berlin, Germany
{menzel,wolisz}@tkn.tu-berlin.de

Abstract. Indicating the imminent battery depletion of wireless sensor nodes is beneficial for many applications. But corresponding depth of discharge estimation approaches are either complex, constraint or rather imprecise. We present, implement and evaluate a novel approach which is to observe the battery's overpotential — the change of the voltage under a load in comparison to the unloaded battery — which increases toward the end of a battery's lifetime. Experimental evidence that the battery's overpotential is a better "end-of-life" indicator than the commonly used operating voltage is provided. Also, it does neither require any additional circuitry in typical sensor nodes nor significant processing overhead.

Keywords: Battery, Overpotential, WSN, End-of-Life Indication, Estimation.

1 Introduction

The vast majority of contemporary wireless sensor networks consist of nodes powered by batteries (this pertains equally to many other devices — including cell phones). Energy harvesting is the promising alternative, but also in these systems, storage is needed to bridge the gap between energy supply and demand due to fluctuation in the ambient physical systems and changing consumption of the node. Here, rechargeable batteries are often preferred over super capacitors due to their smaller size, higher capacity, lower self-discharge and lower price.

Knowing the battery discharge state is essential for energy management. In most use-cases it is, however, most important to predict early enough the approaching node failure due to energy shortage. Such knowledge can be efficiently used to tune the communication protocols so as to "unload" the critical node, it might also trigger reduction of the sensing/ computing activity of the node, e.g. its usage only under critical circumstances.

The established approach to indicate end-of-life of a battery is to measure its voltage and compare it to a predefined threshold value. The voltage curve is, however, dependent on the battery chemistry, details of its design, operation temperature and discharge characteristics. Therefore, for an accurate end-of-life indication, choosing an appropriate threshold requires good knowledge of all the above, which might be hard to obtain in real applications.

M. Zuniga and G. Dini (Eds): S-Cube 2013, LNICST 122, pp. 34–46, 2013.

In this work, we are going to present a novel approach to end-of-life indication in duty-cycled wireless sensor nodes. It is based on observing the overpotential, i.e. the decrease of the voltage under a load in comparison to the unloaded battery. Measurements of the overpotential in common batteries has lead us to the conclusion that overpotential is less prone to variations due to construction and operation parameters than the pure operating voltage, usually used for battery end-of-life prediction. Thus, our approach enables a more precise detection of the imminent battery depletion.

The remaining paper is organized as follows: In Section 2, we discuss the previous work on discharge state estimation, introduce the concept of overpotential and formulate our research hypothesis. In Section 3, we describe our experimental setup. In Section 4, we present and discuss our results. Finally, in Section 5, we conclude the paper and outline some open questions.

2 Previous Work and the Working Hypothesis

During the discharge of an electrochemical battery, its voltage decreases with increasing depth of discharge (DoD) until it falls below the cutoff voltage which defines the battery's end-of-life. Thus, it is quite obvious to derive the DoD from the voltage level. But the actual voltage during a battery's discharge also depends on the time profile of the discharge, the temperature and the cell's past [16, p. 3.1 ff.]. Therefore, in order to obtain good DoD estimation results, purely operating-voltage based estimation requires known and stable battery and discharge characteristics. Different approaches exist to support the consideration of a wider range of discharge rates and patterns, often combined with lifetime prediction, as e.g. in [21].

Those approaches differ firstly in their complexity regarding the used battery models: For example, fixed voltage values have been used as thresholds for DoD categorization in the commercially available Archrock wireless sensor nodes [1]. Polynomial fitting of discharge curves obtained at constant load has been examined in [21] and was further developed in [2]. More accurate, but also more complex are advanced electrochemical [6], analytical [15] and stochastical [4] models.

The methods furthermore depend on a different amount of runtime parameters: Purely bookkeeping of the performed instructions on the software level is performed in [22]. Continuous monitoring of voltage, current and temperature is needed in [14]. The approach aims for accurate replication of the electrochemical processes inside the battery during discharge. The underlying mathematical model is based on more than thirty battery parameters. Those have to be either known or determined by numerical fitting of data obtained by charge and discharge experiments at different modes.

Depending on the chosen approach, voltage, current and/or temperature therefore has to be monitored, often at a highly granular basis. Simultaneously, the obtained values have to be applied to the battery model in order to obtain the DoD estimation. To our knowledge, a comprehensive performance comparison

of existing estimation techniques is pending. Nevertheless, a higher prediction accuracy, respectively a larger flexibility in terms of the application scenario and constraints can be achieved by using the more sophisticated approaches. This challenges an actual implementation on resource-constrained wireless sensor nodes. With [23] and [10] commercially available hardware components performing similar estimation approaches as discussed above are presented. Those are, however, limited to lithium-ion batteries and do also require extensive application and battery characterization (e.g. 13 parameters for [10]).

Thus, accurate DoD estimation is only possible at the cost of high overhead (see e.g. also [13]). In many use cases, there is no need to have a complete DoD estimate — in contrary, it is sufficient to know whether the end-of-life is about to occur in the near future or not. Exactly for this purpose we suggest a novel approach delivering such a binary indication with a higher precision.

Before explaining our a approach let us introduce some basic notions. The voltage of a cell when no load is applied, is the *open-circuit voltage*, while the *operating voltage* is the voltage when a usually drawn current is running through the cell [16, p. 3.2]. The *overpotential* (also: overvoltage or polarization) [16, p. 2.1 f.],[9,11] is the difference between those two voltages. It reflects the electrochemical and physical processes inside the battery and is therefore not constant over time. When charging the operating voltage is higher, when discharging it is lower than the open-circuit voltage. The factors which contribute most to the observable voltage differences are the following: Activation polarization occurs due to limitations of the chemical reactions and the charge transition between the electrolyte and the electrode surface, while concentration polarization arises from concentration differences of the active species in the electrolyte. On the other hand, adsorption polarization, crystallization polarization and reaction polarization do not play this role.

As it is an important effect in electrochemistry, the phenomenon of overpotential is also covered by the earlier mentioned detailed battery models (e.g. [14]). However, we are targeting for one interesting aspect of the overpotential, which is its increase toward the end of the battery's life [3, p.220], [16, p. 2.17]. We investigate the possibility of utilizing this effect for accurate end-of-life indication in a simple manner.

Indication of end-of-life by detecting a voltage drop in continuous discharge as well as the exertion of artificial testing pulses has been proposed for lithium thionyl chloride cells in [18]. However, the motivation for this work comes from the observation that in wireless sensor networks batteries always work in a pulsed discharge mode due to the duty cycling of the nodes. This seems to offer inherently very favorable conditions for the appearance of the overpotential. In this work we first investigate the possibility of measuring the overpotential in commodity WSN nodes. Afterwards we investigate to what extent so achieved values can be used for reliable prediction of the end-of-life for alkaline, nickel-metal hydride an lithium-ion batteries.

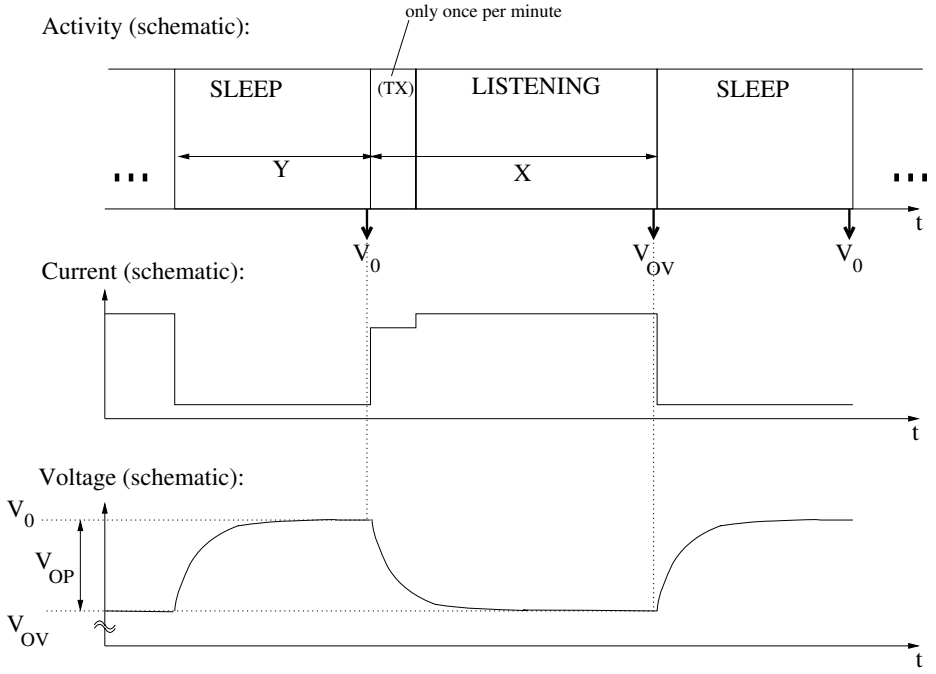

Fig. 1. Duty cycling mote application

3 Experimental Setup

Our investigations are aimed at the usage in typical wireless sensor networks. Nodes are selected to be Tmote Sky motes [12] running under the TinyOS 2.1 operating system. The measurements are sent to a PC-attached base station.

We will compute V_{OP} as the voltage difference between states where low and high current is drawn from the battery. Instead of inducing these changes artificially, we exploit the inherent current pulsing of duty cycling wireless sensor nodes. The mote is running a scheme which is shown in Figure 1. A duty cycle of $D = \frac{X}{X+Y}$ is performed: X seconds with the radio in listening mode are followed by a period of Y seconds with switched-off radio. Once per minute, the gathered voltage and temperature data is sent to the base station.

Our aim is to obtain the battery's overpotential V_{OP}. As introduced in the previous section, it is the difference between the open-circuit voltage and the operating voltage: $V_{OP} = V_0 - V_{OV}$. At V_0, by definition no current is running through the cell. It is therefore rather challenging to have an embedded system measure its open-circuit voltage. Thus, in this work we take the voltage at a very low current as approximation for V_0. Furthermore, we want to maximize the time for the battery voltage to relax to the open-circuit voltage. As illustrated in Figure 1, we therefore take the V_0 measurements shortly before each upcoming current pulse. Due to similar considerations, the V_{OV} measurements are taken

as late as possible during the active phases in order to maximize electrochemical diffusion [16, p. 2.2].

We choose $X = Y = 10\,\text{s}$ resulting in a duty cycle of $D = 50\,\%$. These values do not reflect a typical WSN scenario, but enable us to obtain total lifetimes of several days up to a couple of weeks using commercially available batteries. However, even longer rest periods at smaller duty cycles would not reduce the difference between our measured V_0 the real open circuit voltage significantly, since the relaxation occurs logarithmically (see [16, p. 3.12], illustrated in Figure 1). We also assume the duration of current pulses to be long enough to sufficiently release the exponentially growing overpotential effect. Still, it is an important open question to identify a lower bound on the pulse duration and the discharge current.

We use different types of batteries with different nominal voltages and capacities as shown in Table 1.

Table 1. Battery Types which are used in this work

type	name	nom. voltage	nom. capacity	rechargable	ref.
Alkaline	Varta 4106	1.5 V	2600 mAh	no	[19]
NiMH1100	Conrad NiMH 1100	1.2 V	1100 mAh	yes	[5]
NiMH800	Varta 46736	1.2 V	800 mAh	yes	[20]
LiIon	Emmerich LiFePho 18650	3.3 V	1100 mAh	yes	[8]

While it is sufficient to use a single LiIon cell, Alkaline and the NiMH batteries are used pairwise in order to obtain a voltage level usable for the Tmote Sky. During our experiments, we use 8 (12, 4, 3) pieces of the Alkaline (NiMH1100, NiMH800, LiIon) batteries. NiMH1100 cells are charged with the ELV ALM 7003 charger [7] using a current of 100 mA (NiHM800: 80 mA). LiIon cells are charged with the iMAX B6AC [17] at 1500 mA.

Most of the experiments are run at temperatures of 20 °C to 25 °C. A fridge is used to perform experiments at temperatures of about −10 °C to 0 °C. The unused space is filled with styrofoam in order to reduce the temperature variation due to the thermostat cycling. We use a halogen lamp to run experiments at about 35 °C to 40 °C.

Tmote Sky allows to measure half of the battery voltage in either a range from 0.75 V to 1.5 V or from 1.25 V to 2.5 V. Our used batteries operate in the range from about 1.5 V to 3.4 V resulting in a needed measuring range from 0.75 V to 1.7 V. We therefore perform all voltage measurements with both references. The proper range is finally evaluated offline.

4 Evaluation

We present results of evaluating the battery discharge curves obtained during 82 experiments each running from 3 to 14 days. In order to aggregate the individual runs and to enable comparison of the different durations, all curves are normalized to DoD.

Due to various reasons (e.g. human failure on starting the data logging, power cut but also when reaching operating voltages too close to the lower measurement reference of 1.5 V) there are occasional holes in the individual voltage traces. An important aspect of our evaluation is going to be the estimation of confidence intervals (CIs). Those are quite sensitive to changes in the number of observations. Therefore, in order to prevent distortion, such periods with a reduced number of valid traces are excluded by our data processing. They can easily be identified as gaps in the presented curves which have data points for all DoD $\in [0, 1]$ in the absence of such holes.

If not stated otherwise, we are commenting the experiments which have been performed at room temperature. All presented calculations and presented curves are based on a moving average on the raw voltage measurements of 30 min.

4.1 Overpotential toward End-of-Life

To give a first overview, Figure 2 shows the average operating voltage V_{OV} and the overpotential V_{OP} of the evaluated battery types. Most notably, this proves that it is possible to observe overpotential without adding further measuring circuitry in duty cycled sensor nodes.

Figure 3 highlights the last 10 % of the batteries' lifetimes, as we are mainly interested in this phase. As a first result we find that toward the end of the batteries' lifetimes V_{OV} decreases as commonly known. But also, as predicted in Section 2, we can verify that V_{OP} strongly increases when approaching DoD of 1.

For simple end-of-life indication, we seek a proper threshold value. Such a value could reasonably be chosen in the region where V_{OP} is rising (e.g., here, DoD> 0.99). Assuming a constant variability, one can expect more precise indication at higher slopes of V_{OP}. Whereas defining a similar lower threshold based on operating voltage would require more effort due to the flatter curves, higher and different offsets.

4.2 Overpotential versus Operating Voltage Variability

In order to compare the variability of V_{OP} and V_{OV}, we plot the width of the 95 % CI assuming Student's t-distribution in Figure 4. In Table 2 the average widths of the CIs are summarized. For all evaluated battery types the overpotential's CI is smaller than the corresponding value for the operating voltage. Therefore we claim that our experiment indicates the superiority of the end-of-life indication for the given battery types if overpotential thresholds are used rather than operating voltage thresholds. For example, with 25 mV, V_{OP}'s CI at 90 % DoD is only half as wide as V_{OV}'s 50 mV.

As V_{OV} is the actual seen battery voltage, its variability defines a lower bound on the accuracy of the battery voltage models introduced in Section 2.

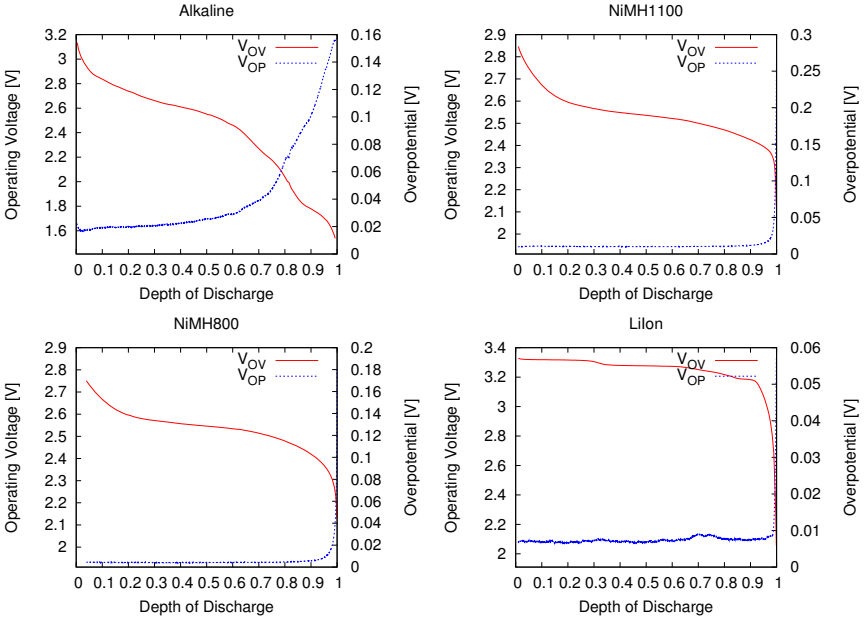

Fig. 2. Operating voltage and overpotential during the discharge of the different batteries (average over n individual runs, $n_{Alkaline} = 4, n_{NiMH1100} = 20, n_{NiMH800} = 7, n_{LiIon} = 7$)

4.3 Temperature Dependency

We evaluate the robustness of V_{OV} and V_{OP} on the variation of the ambient temperature. For each battery type, the average curves for normal, high and low temperature of both, V_{OV} and V_{OP} are plotted jointly in Figure 5. As we are mainly interested in the end phase of the batteries' lifetimes, we use an exponential scale on the x-axes. The y-axes on each subfigure use the same scale. This enables direct comparison of the two approaches as both values are technically obtained by the same voltage measuring circuit. V_{OP}, which we propose in this work, is less influenced by changes in the ambient temperature than V_{OV}. Also,

Table 2. Average width of operating voltage's and overpotential's 95 % confidence interval

	entire lifetime		last 10 %	
	$V_{OV}[V]$	$V_{OP}[V]$	$V_{OV}[V]$	$V_{OP}[V]$
Alkaline	0.070	0.008	0.129	0.019
NiMH1100	0.065	0.004	0.038	0.011
NiMH800	0.188	0.002	0.121	0.011
LiIon	0.044	0.005	0.108	0.007

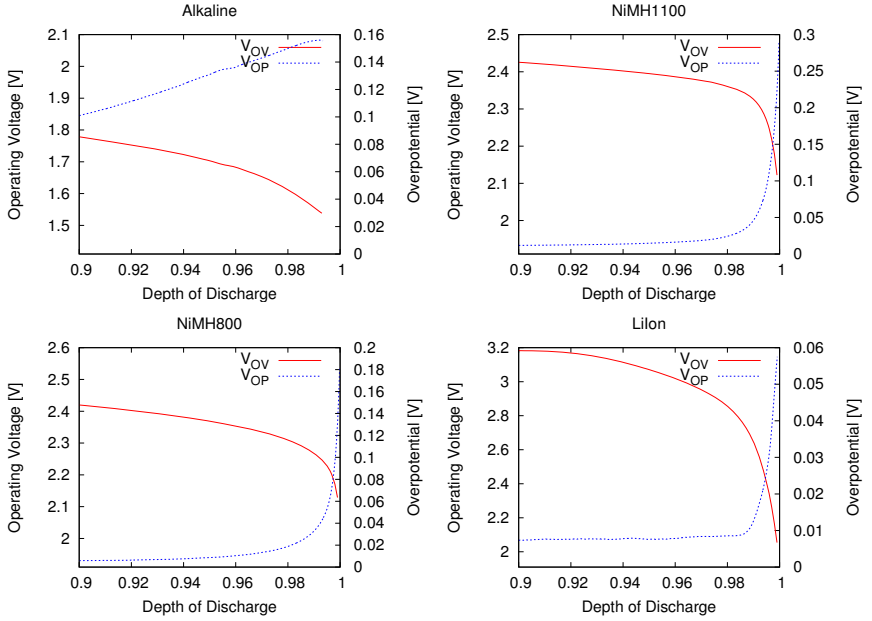

Fig. 3. Operating voltage and overpotential during the last 10 % of battery lifetime

for warm and cold ambient conditions, V_{OP} varies less than V_{OV} as summarized in Table 3.

End-of-life indication based on obtaining the battery's overpotential is thus more robust to temperature variations than operating voltage based indication.

Table 3. Average CI-widths in warm and cold environment

	warm $(35 - 40\,^{\circ}\mathrm{C})$		cold $(-10 - 0\,^{\circ}\mathrm{C})$	
	$V_{OV}[V]$	$V_{OP}[V]$	$V_{OV}[V]$	$V_{OP}[V]$
Alkaline	0.059	0.012	0.164	0.040
NiMH1100	0.063	0.026	0.076	0.017
NiMH800	0.148	0.008	0.025	0.003
LiIon	0.045	0.002	0.057	0.004

4.4 End-of-Life Indication without Knowledge of the Battery Type

Whenever a WSN node's battery is not integral with the device, it is quite likely that other than the initially deployed batteries are eventually used. Especially, as consumer market sensor nodes like [1] come with standard battery holders.

We therefore evaluate V_{OV} and V_{OP} for their ability to indicate the approaching end-of-life in the absence of knowledge of the battery type.

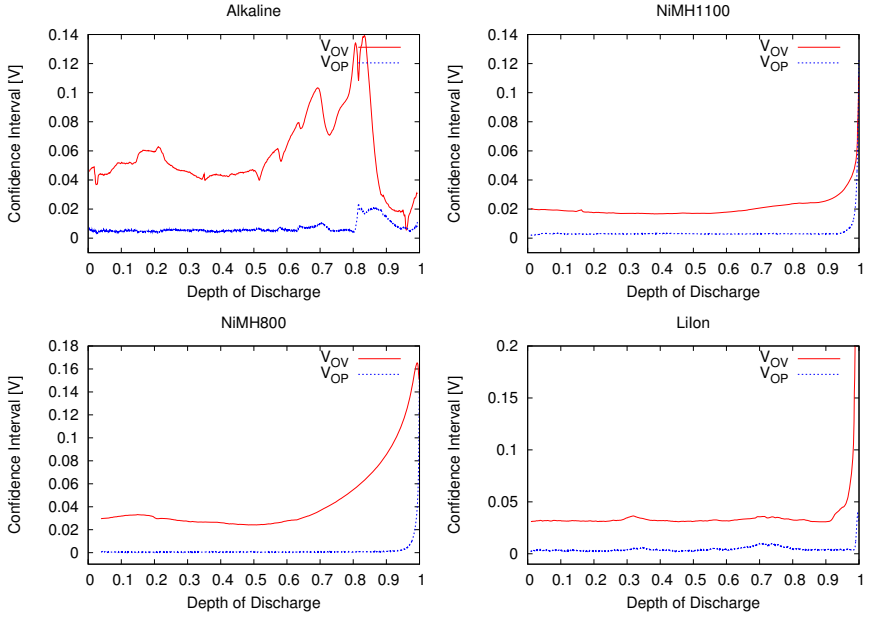

Fig. 4. Width of operating voltage's and overpotential's 95 % confidence interval assuming a Student's t-distribution

In Figure 2 and 3, the operating voltages of all evaluated battery types have been shown jointly. The curves differ in position and slope which impedes to define a common voltage threshold that could be established as end-of-life indicator. For LiIon, a threshold higher than 2.4 V would be suitable, NiMH required a little below 2.4 V and Alkaline a value less than 2.0 V.

Also the observed overpotential curves have been presented in Figure 2. For each battery type, V_{OP} increases toward the end of the lifetime. A threshold of 0.1 V is crossed within the last 90 % of three of the batteries' lifetimes. However, the LiIon battery never reaches that value.

In Figure 2, for most of the battery types different, but rather constant offsets can be identified. To eliminate these, we extend our approach by dividing V_{OP} by the minimal value that has been observed until then during each measurement. This normalization does increase only minimal overhead and could be easily implemented on a resource constrained WSN node. The obtained curve is shown in Figure 6. While Alkaline still shows an earlier but slower rise than the other, it nevertheless is possible to establish a ratio of about 6 as a threshold to indicate that at least 90 % (but less than 100 %) of the battery's capacity is spent without knowing the chosen battery type. We want to highlight, that a similar statement is not to obtain by sole monitoring of the operation voltage.

To prove that also a threshold resulting in indication at DoD levels of close to 1 can be still useful, we consider a simple temperature monitoring application. When choosing a $V_{OP}/MIN(V_{OP})$ ratio of 6, the mote including the radio can be

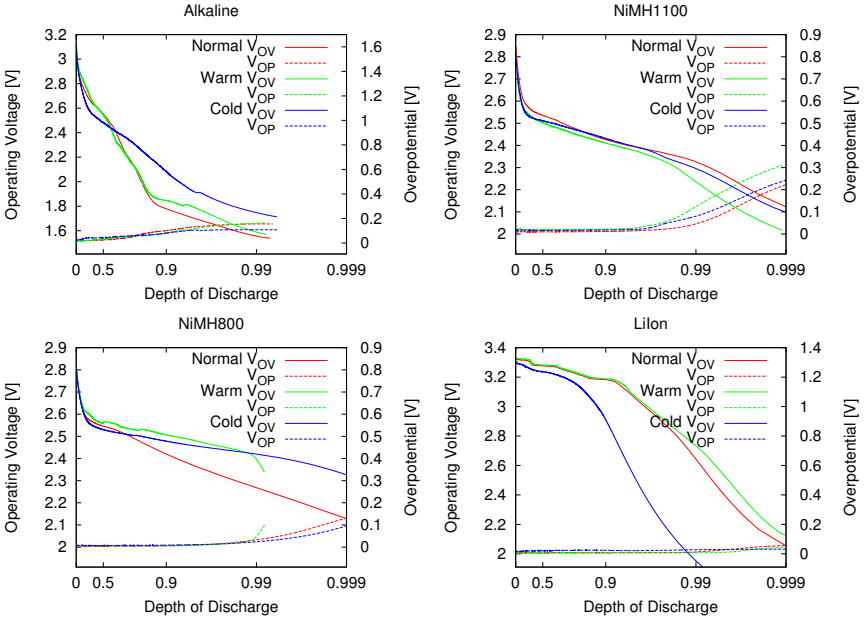

Fig. 5. Operating voltage (left, declining) and overpotential (right, rising) during the discharge at room temperature, warm and cold conditions, Alkaline: ($n_{normal} = 4, n_{warm} = 4, n_{cold} = 4$); NiMH1100: (20, 8, 11); NiMH800: (7, 3, 5); LiIon: (7, 5, 4)

operated continuously for about 0.2 h when using the LiIon battery (NiMH1100: 0.5 h, NiMH800: 0.8 h, Alkaline: several hours) after crossing this threshold. As these durations can be expanded by duty cycling, this amount of remaining lifetime should be sufficient to e.g. request for battery exchange or in more complex applications to reconfigure the network or to complete any pending operations safely.

We also evaluate the robustness of $V_{OP}/MIN(V_{OP})$ on the variation of the ambient temperature. To obtain the same 90 % DoD indication we find that for warm batteries the same threshold ratio of 6 can be used, while this value has to be reduced to 4 for cold batteries. Thus, this approach is not temperature agnostic which consists with our findings in Section 4.3. However, with additional temperature knowledge the approach can also be used in this case.

5 Conclusions

We introduced a novel approach for indicating the end-of-life of batteries operated in a duty cycled mode — the overpotential-based end-of-life indication. The approach has been implemented and evaluated in 82 experiments using Tmote Sky sensor nodes and 4 different types of batteries at different ambient temperatures. Firstly we showed that for any known battery type it is possible to

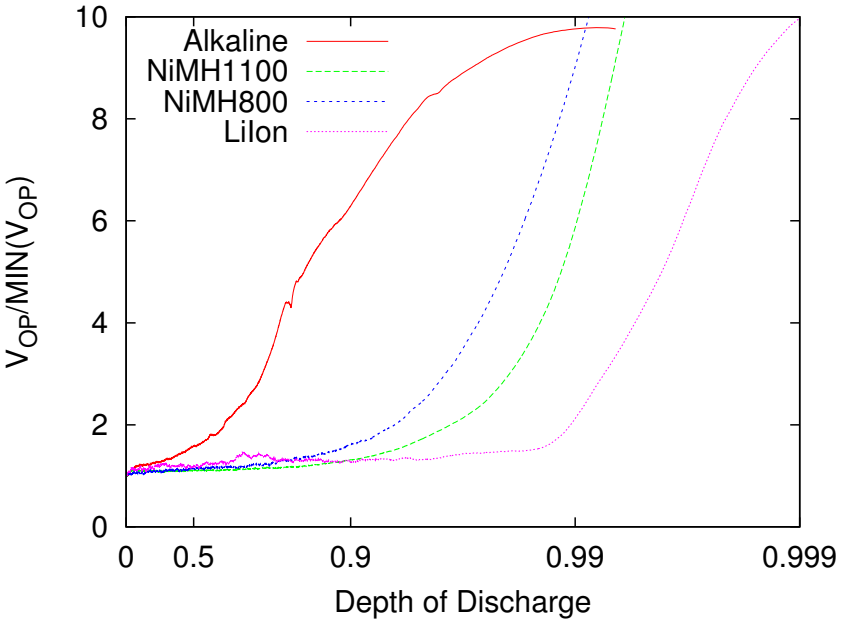

Fig. 6. Overpotential divided by its so far minimal value

observe and utilize overpotential in duty cycled sensor node applications without additional circuitry. The sharp increase of the overpotential toward the end of the batteries' life recommends its utilization for end-of-life indication. The experiments then proved that the overpotential varies less over depth of discharge than the operating voltage which allows to select overpotential thresholds in a way assuring more precise end-of-life indication than by using operating voltage thresholds. This does also hold at increased and reduced ambient temperature.

Consider the following use-case: A cluster head node is supposed to initiate the election of a successor shortly before its end-of-life. It would be possible to apply one of the arbitrary complex operating voltage based models mentioned in Section 2 or perform some measurements in order to define a proper operating voltage threshold. Alternatively, some measurements could be used to identify a suitable overpotential threshold. As shown in this work, the overpotential based indication would result in higher accuracy. However — and that is our approach's limitation — due to the flat overpotential curve, it is not possible to use overpotential for indication of random DoD levels.

In addition we have addressed the issue of end-of-life indication without knowledge of the battery type. Pure operating voltage based indication is hardly possible at all for this case. We have demonstrated that the overpotential based approach can be applied successfully also in this case. This opportunity is best used by putting overpotential into relation to the minimum level observed during the operation in the given operational environment. Albeit the prediction

achieved without battery type knowledge is not really precise, we claim that this indication might be useful in practical cases.

As the increase of the overpotential toward the battery's complete depletion is a know effect, similar results for other than the evaluated battery types and chemistries can be expected.

We have focused here on the end-of-life estimation only, as we consider this information to be most important for reliable usage of the WSNs in many applications. Obviously, if some information about the ongoing level of discharge might be needed, a combination of our approach for end-of-life detection with the observation of the operational voltage for the sake of the ongoing discharge monitoring might be attractive.

References

1. Arch Rock Corporation: Primer Pack User Manual, http://www.mediamob.co.kr/FDS/newBlogContent/2007/0406/infoland/primerpack_datasheet.pdf
2. Buchli, B., Aschwanden, D., Beutel, J.: Battery state-of-charge approximation for energy harvesting embedded systems. In: Demeester, P., Moerman, I., Terzis, A. (eds.) EWSN 2013. LNCS, vol. 7772, pp. 179–196. Springer, Heidelberg (2013)
3. Bergveld, H.J.: Battery management systems: design by modelling. Ph.D. thesis, University of Twente, Enschede (June 2001)
4. Chiasserini, C.F., Rao, R.R.: Improving battery performance by using traffic shaping techniques. IEEE Journal on Selected Areas in Communications 19(7), 1385–1394 (2001)
5. Conrad Electronic SE: Datasheet nimh100, http://www.produktinfo.conrad.com/datenblaetter/250000-274999/250025-da-01-en-Voltcraft_NiMH_Mignon_Akkuset.pdf
6. Doyle, M., Fuller, T.F., Newman, J.: Modeling of galvanostatic charge and discharge of the lithium/polymer/insertion cell. Journal of the Electrochemical Society 140(6), 1526–1533 (1993)
7. ELV Elektronik AG: Alm 7003 akku-lade-messgert, http://www.elv-downloads.de/service/manuals/ALM7003/ALM7003_UM_G_020417.pdf
8. Emmerich Energy GmbH: Lifepho 18650, http://www.produktinfo.conrad.com/datenblaetter/250000-274999/250796-da-01-en-LiFePO_4_AKKU_ULT
9. Jossen, A., Weydanz, W.: Moderne Akkumulatoren richtig einsetzen. Inge Reichardt Verlag, Untermeitingen (2006)
10. Maxim Integrated: Datasheet max17047/max17050 modelgauge m3 fuel gauge
11. Menzel, T., Willkomm, D., Wolisz, A.: Improving battery-efficiency of embedded devices by favorably discharging only towards end-of-life. In: Proc. of the CONET 2011 Workshop, Chicago, USA (April 2011)
12. Moteiv Corporation: Tmote Sky Datasheet, http://www.snm.ethz.ch/snmwiki/pub/uploads/Projects/tmote_sky_datasheet.pdf
13. Pop, V., Bergveld, H., Danilov, D., Regtien, P., Notten, P.: Battery Management Systems: Accurate State-of-Charge Indication for Battery-Powered Applications. Philips Research Book Series 9. Springer, London (2008)
14. Pop, V., Bergveld, P., Het Veld, J.H.G.O., Regtien, P.P.L., Danilov, D., Notten, P.H.L.: Modeling battery behavior for accurate state-of-charge indication. Journal of the Electrochemical Society 153, A2013–A2022 (2006)

15. Rakhmatov, D., Vrudhula, S., Wallach, D.A.: Battery lifetime prediction for energy-aware computing. In: ISLPED 2002: Proceedings of the 2002 International Symposium on Low Power Electronics and Design, pp. 154–159. ACM Press, New York (2002)
16. Reddy, T.B., Linden, D. (eds.): Linden's Handbook of Batteries, 4th edn. McGraw-Hill (2010)
17. SkyRCTechnology: Datasheet b6ac, http://www.skyrc.com/index.php?route=product/product&keyword=imax%20b6ac&product_id=10
18. Tadiran Batteries GmbH: Tadiran Lithium Batteries, Technical Brochure
19. Varta AG: Datasheet battery no. 4106, http://www.varta-microbattery.com/applications/mb_data/documents/data_sheets/DS4106.PDF
20. Varta AG: Datasheet battery no. 56736, http://litel.com.pl/attachments/File/Akumulatory_konsumenckie/Varta/AA_800.pdf
21. Wen, Y., Wolski, R., Krintz, C.: Online prediction of battery lifetime for embedded and mobile devices. In: Falsafi, B., VijayKumar, T.N. (eds.) PACS 2003. LNCS, vol. 3164, pp. 57–72. Springer, Heidelberg (2004)
22. Ye, C.K.: Application-level prediction of battery dissipation, http://citeseer.ist.psu.edu/719497.html
23. Yu, M., Barsukov, Y., Vega, M.: Theory and implementation of impedance track battery fuel-gauging algorithm in bq2750x family. Tech. rep., Texas Instruments Incorporated (2008)